

This is a pre print version of the following article:

Organ culture and Reflectance Confocal Microscopy as new integrated tools for barrier rescue studies in inflammatory skin diseases / Petrachi, Tiziana; Lotti, Roberta; Palazzo, Elisabetta; Truzzi, Francesca; Saltari, Annalisa; Morandi, Paolo; Ciardo, Silvana; Pellacani, Giovanni; Pincelli, Carlo; Marconi, Alessandra. - In: EXPERIMENTAL DERMATOLOGY. - ISSN 0906-6705. - ELETTRONICO. - 24:12(2015), pp. 980-982. [10.1111/exd.12823]

Terms of use:

The terms and conditions for the reuse of this version of the manuscript are specified in the publishing policy. For all terms of use and more information see the publisher's website.

09/01/2026 11:51

Organ culture and Reflectance Confocal Microscopy as new integrated tools for barrier rescue studies in inflammatory skin diseases

Journal:	<i>Experimental Dermatology</i>
Manuscript ID:	EXD-15-0099
Manuscript Type:	Regular Article
Date Submitted by the Author:	20-Feb-2015
Complete List of Authors:	<p>Petrachi, Tiziana; University of Modena and Reggio Emilia, Department of Surgical, Medical, Dental and Morphological Sciences</p> <p>Lotti, Roberta; University of Modena and Reggio Emilia, Department of Surgical, Medical, Dental and Morphological Sciences</p> <p>Truzzi, Francesca; University of Modena and Reggio Emilia, Department of Surgical, Medical, Dental and Morphological Sciences</p> <p>Saltari, Annalisa; University of Modena and Reggio Emilia, Department of Surgical, Medical, Dental and Morphological Sciences</p> <p>Morandi, Paolo; University of Modena and Reggio Emilia, Department of Surgical, Medical, Dental and Morphological Sciences</p> <p>Ciardo, Silvana; University of Modena and Reggio Emilia, Department of Surgical, Medical, Dental and Morphological Sciences</p> <p>Pellacani, Giovanni; University of Modena and Reggio Emilia, Department of Surgical, Medical, Dental and Morphological Sciences</p> <p>Pincelli, Carlo / Editorial Board Member; University of Modena and Reggio Emilia, Dermatology;</p> <p>Marconi, Alessandra; University of Modena and Reggio Emilia, Department of Surgical, Medical, Dental and Morphological Sciences</p>
Keywords:	skin barrier, RCM, Tape stripping, SDS , barrier repair

**Organ culture and Reflectance Confocal Microscopy as new integrated tools for barrier
rescue studies in inflammatory skin diseases**

Tiziana Petrachi¹, Roberta Lotti¹, Elisabetta Palazzo¹, Francesca Truzzi¹, Annalisa Saltari¹, Paolo Morandi¹, Silvana Ciardo², Giovanni Pellacani², Carlo Pincelli¹ and Alessandra Marconi^{1*}

¹Laboratory of Cutaneous Biology, Department of Surgical, Medical, Dental and Morphological Sciences, University of Modena and Reggio Emilia, Modena, Italy
²Dermatology Unit, Department of Surgical, Medical, Dental and Morphological Sciences University of Modena and Reggio Emilia, Italy

*Corresponding author:
Alessandra Marconi
Laboratory of Cutaneous Biology, Department of Surgical, Medical, Dental and Morphological Sciences, University of Modena and Reggio Emilia, via del Pozzo 71, 41124 Modena, Italy.
Tel: +33 059 4222812; Fax: +33 059 4224271; E-mail: alessandra.marconi@unimore.it

Word count: 3974
Number of display: 4

Keywords: Skin barrier, RCM, tape stripping, SDS, barrier repair

For Review Only

1
2
3
4
5
6
7
8
9
10
11
12
13
14
15
16
17
18
19
20
21
22
23
24
25
26
27
28
29
30
31
32
33
34
35
36
37
38
39
40
41
42
43
44
45
46
47
48
49
50
51
52
53
54
55
56
57
58
59
60

ABSTRACT

Epidermal barrier represents the first line of defense against a variety of external insults and its disruption is involved in common inflammatory skin diseases, including psoriasis, contact and atopic dermatitis. Despite a growing interest in skin barrier abnormalities, few studies permit to follow the barrier repair mechanisms. Here we present a new integrated approach to understand skin barrier recovery after physical (tape stripping, TS) or chemical (SDS) injury by combining human skin organ culture and Reflectance Confocal Microscopy (RCM). TS *in vitro* produced a complete removal of stratum corneum and lipids, a drastic decrease of structural and adhesion proteins, and an increase in cell proliferation. Epidermal recovery with either proliferation or differentiation rescue was observed after 18 hours, with no apoptotic cell detection. On the other hand, when skin organ cultures were exposed to 2% SDS, cellular junctions were disrupted and the expression of late differentiation markers decreased. Junctions repair was detected 24 hours after treatment, with the restoration of epidermal integrity. Both models (TP or SDS) showed the induction of immune-inflammatory markers, such as psoriasin, keratin 16, and the increase in Langerhans cell number. RCM confirmed all the morphological and structural features presented by the organ cultures, thus making this technique fast and easily applicable in the context of dermatological research. These results indicate that combination of skin organ models and RCM can be successfully used for the study of barrier perturbation in skin diseases, for toxicology tests, and for evaluating novel therapies.

INTRODUCTION

Skin protects the body against microbiological infection, mechanical and chemical stress. Skin impermeability is ensured by the integrity of the outermost keratinocyte layer, the stratum corneum (SC), in which protein rich corneocytes are embedded in a lipid rich intercellular space (1). Corneodesmosomes hold keratinocytes together, and undertake a gradual degradation process leading to desquamation (2). Adherents and tight junctions contribute to barrier functions, by mediating intercellular stability, protecting the organism from the outside and by preventing water loss (3).

Barrier alteration is associated with desquamation, loss of corneocyte cohesiveness and extracellular lipids content, increasing transepidermal water loss (TEWL) and skin dehydration (4). Upon artificial barrier disruption, basal keratinocyte proliferative kinetics is accelerated in mice (5, 6), and the delicate balance between cornification and desquamation is temporarily altered, resulting in hyperkeratosis and parakeratosis (7). However, the knowledge regarding the mechanisms underlying the repair of the barrier is still sparse and incomplete.

Experimentally disrupted skin barrier is extensively used not only to study epidermal regeneration after injury, but also to quantify topical and transdermal drug penetration (8) or to evaluate drug bioavailability and bioequivalence. Experimental methods to perturb permeability barrier include tape stripping (TS), as a mechanical approach of SC removal (9), and the application of irritant and/or chemical substances on the skin surface in vivo, such as acetone, detergents, sodium dodecyl sulphate (SDS) (4). Initial in vitro studies were mostly focused on biochemical assessments, such as TEWL or pH determination (10). In addition, to avoid subjecting patients to unnecessary discomfort and risk, the experimental damage induction in humans must be mild and poorly invasive (11). However, this approach only partially alters or removes the SC, therefore limiting the studies on barrier perturbation. Several studies were performed in animal models such as mice, dog and pig (12, 13, 14), although results must take into account the interspecies difference (15, 16).

1
2
3
4
5
6
7
8
9
10
11
12
13
14
15
16
17
18
19
20
21
22
23
24
25
26
27
28
29
30
31
32
33
34
35
36
37
38
39
40
41
42
43
44
45
46
47
48
49
50
51
52
53
54
55
56
57
58
59
60

Reflectance confocal microscopy (RCM) has opened a new imaging era, giving clinicians the opportunity to analyze architectural and cytological features at nearly histological resolution in vivo (17, 18, 19), overcoming limitations of traditional microscopy, such as the need of biopsy and processing before visualization (20, 21, 22). RCM, based on their refractive index, analyzes in vivo big areas of the skin, and allows to evaluate in detail all epidermal layers, the dermis, blood flow and rete ridges (23), as well as the dermo-epidermal junction (24). RCM has been used as a support for the diagnosis of several skin diseases, such as psoriasis (25), actinic keratoses (26), sebaceous gland hyperplasia (27, 25), allergenic contact dermatitis (28, 29), and skin cancer (30, 31). Recently, RCM aspects of dry skin and changes occurring during the hydration given by moisturizers showed the applicability of this technique to in vivo monitoring of morphological variations of keratinocytes and inter-keratinocyte junctions related with skin barrier function (32). Given that common inflammatory skin diseases (e.g. psoriasis and atopic dermatitis) show skin barrier abnormalities (33), the study of skin barrier recovery is of great value.

Here, we used in vivo human skin organ culture models to disrupt skin barrier through TS or SDS exposition. We demonstrate that our systems faithfully reproduce in vivo conditions of barrier perturbation and repair, showing a gradual and slow return to normal proliferation and differentiation over time. In addition, RCM accurately correlates with morphological and functional aspects obtained by traditional techniques. The combination of skin organ cultures and RCM offers a new exciting approach to study in vitro barrier perturbation by testing the efficacy of barrier repair drugs and allowing the execution of fast, non invasive toxicological studies.

MATERIAL AND METHODS

Skin organ culture model of barrier perturbation by tape stripping (TS) or SDS treatment

Skin organ cultures were generated by 8mm-punch biopsies from healthy skin obtained from waste materials from Operating Room by. Patient consent for experiments was not required because Italian laws consider human tissue left over from surgery as discarded material. For the TS model, 40, 60 and 100 repeated 3M adhesive tape applications and removal were applied on total skin to remove SC (Fig. S1). Biopsies were maintained in air-liquid interface and analyzed at different time points after TS treatment (0, 18, 24 and 36 hours). For the SDS model, organ culture were treated with 2% SDS and incubated at 4°C for 18 hours, before starting culturing in air-liquid interface (Fig. S1). They were analyzed at different time points after SDS treatment (0, 18, 24 and 36 hours). For both models, the longest time point untreated air-liquid cultured skin biopsy was used as control. Epidermal thickness was measured by ImageJ software. In addition, TS model was further tested by the application of a barrier recovery cream on skin organ cultures immediately after TS treatment, and the barrier repair was analyzed 18 and 24 hours later. The experiments were done in triplicate and results are displayed as mean \pm SD.

Red oil O staining

Skin organ culture cryosections were dried at room temperature and fixed in ice cold 10% formalin for 5 minutes. After 5 minutes incubation in absolute propylene glycol, slides were stained in pre-warmed Oil Red O solution (Sigma, St. Louis, MO, USA) for 10 minutes at 60°C, differentiated in 85% propylene glycol solution and counterstained with Mayer's hematoxylin for 30 seconds. The images are representative of three independent experiments.

Immunohistochemistry

Skin organ culture sections from formalin fixed-paraffin blocks were stained using the UltraVision LP Detection System AP Polymer & Fast Red Chromogen assay (Thermo Fisher Scientific),

according to the manufacturer's instructions. Briefly, slides were treated with Ultra V Block and samples were incubated with polyclonal rabbit anti-loricrin (1:500 Abcam) or monoclonal mouse anti-filaggrin (1:50, Abcam); or polyclonal rabbit anti-claudin 1 (ready to use, Abcam), or monoclonal rabbit anti-ki67 (1:100, Epitomics), or monoclonal rabbit anti-P-Stat3, mouse anti-keratin 16, polyclonal rabbit anti-psoriasin, monoclonal rabbit anti-CD1a (ready to use, Ventana) for 1 hour at room temperature. After washes in PBS, Primary Antibody Enhancer (Thermo Fisher Scientific) was added for 20 minutes at room temperature, followed by incubation with AP Polymer anti-mouse/rabbit IgG for 30 min at room temperature. Slides were stained with Fast Red using Naphthol Phosphate as substrate. Samples were analyzed under a conventional optical microscope (Zeiss Axioskope 40). The results were scored according to entities and intensity of expression: - not expressed; + poorly expressed; ++ moderately expressed; +++ well expressed. The images are representative of three independent experiments.

Immunofluorescence

Skin organ culture sections from formalin fixed-paraffin blocks were blocked with a 0,5% BSA/ 5% goat serum solution for 15 minutes. Slides were then incubated for 1 h at 37°C with polyclonal rabbit anti-claudin 1 (1:100, Abcam) or anti-desmoglein 1 (1:100; Santa Cruz). The corresponding TRITC-conjugated secondary antibodies were added in the dark for 45 minutes at room temperature and were analyzed by confocal microscopy (Leica TCS SP2; Leica, Heerbrugg, Switzerland). The images are representative of three independent experiments.

Western Blotting

Total proteins were extracted with RIPA lysis buffer containing protease inhibitors. Equal amount of protein from each sample was run through a 10-15% SDS-PAGE gel and transferred onto a nitrocellulose membrane. Briefly, membranes were first incubated in blocking buffer and then overnight at 4°C with the following primary anti-human antibodies: polyclonal rabbit anti-caspase 3

(1:1000, Cell Signalling), anti-desmoglein 1 (1:200, Santa Cruz), anti claudin 1 (1:25, Abcam), monoclonal mouse anti-involucrin (1:6000, Sigma), anti-desmoglein 3 (1:200, Santa Cruz), anti-filaggrin (1:1000, Abcam), anti- β -actin (1:3000, Sigma), anti-vinculin (1:400, Sigma). After 3 washes with a PBS/tween solution, membranes were incubated with secondary antibodies for 45 min at room temperature. Membranes were washed and developed using the ECL detection system (Amersham Biosciences UK Limited, Little Chalfont Buckinghamshire, U.K). The experiments were done in triplicate and the displayed images are representative of the results.

TUNEL assay

Skin samples were fixed in 4% buffered formalin and embedded in paraffin. Paraffin sections were processed for TUNEL assay using the “In situ cell death detection kit” (In Situ Cell Death Detection Kit, AP; Boehringer Mannheim, according to the manufacturer’s instructions). The labeled DNA was examined by Confocal Scanning Laser Microscopy (Leica TCS SP2 with AOBS) in conjunction with a conventional optical microscope. The images are representative of three independent experiments.

Confocal Reflectance Laser Microscopy

A commercially available reflectance confocal microscope (VivaScope 3000®, MAVIG GmbH, Munich, D) was used for imaging. RCM images were acquired using a standardized protocol for each sample. The protocol included the acquisition of a series of 3 consecutive sequences of images (Vivastack®, Caliber ID, Rochester, NY, USA) starting from the surface up to 150 μ m of depth with a step of 5 μ m. Any single image visualizes an area of 0.8 by 0.8 mm (1000 x 1000 pixels, grey-scale of 256 pixels) enabling a lateral resolution of approximately 1 μ m. RCM descriptors used in these papers derived from the literature (28, 29, 32, 34).

RESULTS

Stratum corneum recovering after complete barrier removal by TS

To ensure a complete SC elimination, we performed a variable number of tape applications (40, 60 and 100) onto total skin from different age and anatomic sites derived from surgical waste and evaluated the epidermal thickness at different time points after skin organ culture (0, 18, 24 and 36 hours) (Fig. S2a,b,c). 100 times of tape repeated applications resulted in barrier disruption, characterized by complete SC removal, as shown by H&E staining (Fig. S2a,b). Indeed, 18 hours after TS, SC started recovering the underneath layers, with a progressive increase in the epidermal thickness that become close to the un-stripped control at 36 hours (Fig. 2c). Therefore, for subsequent studies, we used the TS model with 100 strips, which eliminate the SC without causing apparent morphological alterations of the remaining skin layers.

Intercellular lipid component, known as important regulator of skin permeability (35), was entirely removed after TS treatment, and its regeneration was still undetectable at 36 hours, as shown by Red Oil O dye (Fig. 1a,b). Filaggrin and loricrin, two major proteins expressed in the intact horny layer (36), were markedly impaired after TS. Filaggrin was still poorly detectable 18 hours later, but started to be moderately re-expressed at 24 hours. On the contrary, appreciable levels of loricrin were already detectable at the first time point (Fig. 1a,b).

TS skin application provokes cell-cell junction alteration (37). Therefore, we examined this aspect through the analysis of claudin, a tight junctions-forming protein that is homogeneously expressed in the stratum granulosum (SG). After TS, claudin pattern expression appeared discontinuous and irregular, while it started to reconstitute after 24 hours, reaching levels similar to control at 36 hours (Fig. 1a,b).

By looking more in detail at the differentiation markers, we found that filaggrin expression increased over time, showing higher amounts compared to the untreated control, starting from 18 hours. Involucrin slightly decreased after TS and started to increase at 18 hours. At 24 hours, both filaggrin and involucrin expression was higher than controls (Fig. 1c,d). With a similar profile, the

adhesion molecule desmoglein 1 (Dsg1) was markedly reduced after TS and overexpressed during barrier recovery at 18 and 24 hours as compared to control (Fig. 1c,d).

Increased keratinocyte proliferation during barrier recovery after TS treatment

It has been previously shown that murine barrier perturbation by TS stimulates keratinocyte proliferative kinetics and epidermal hyperplasia (6). To evaluate if the barrier recovery was associated with proliferation or hyperplastic response in our model, we evaluated Ki67 expression and Stat3 phosphorylation (P-Stat3), respectively, at different time points after TS. Interestingly, skin organ cultures responded to barrier damage by increasing proliferation (Fig. 1a). Indeed, they highly expressed Ki67 with a peak at 18 hours post TS when compared to the untreated controls (Fig. 1e). P-Stat3 positive cells were around 100 fold more numerous than in the untreated controls at 18 hours (Fig. 1e) and remained persistently active even at later time points, while Ki67 expression was progressively normalized.

We also addressed if TS-related damage induced keratinocyte apoptosis by TUNEL assay. Few apoptotic cells were detected in the epidermis immediately after TS at 18 hours, most likely due to the presence of parakeratosis caused by the treatment and the activation of terminal differentiation enzymes (38) (Fig. S3a). On the other hand, no dead cells were present at later time points and this result was confirmed by the absence of caspase-3 activation after TS (Fig. S3b).

RCM reveals morphological aspects of skin and barrier repair in TS model

To better define skin barrier recovery after TS, we evaluated skin organ culture morphology by RCM, as integrated imaging technology to analyze barrier perturbation models in vitro. The acquisition of a series of 3 consecutive sequences of images reaching 150 μm depth showed that, immediately after TS, skin organ culture was thinner than control (technical data) and cell contours displayed an irregular pattern, as sign of structural alteration (Fig. 1f). In details, corneocytes were reduced and the honeycombed pattern of the granulosum layer was visible in the upper images. At

1
2
3 18 hours, corneocytes returned to a well defined pattern, while the spinous and granular layer
4 became thicker, thus indicating reactive proliferation. 24 hours after TS, cell contours appeared
5 brighter, most likely because of the intense metabolic activity in response to the barrier damage.
6
7 Finally, at 36 hours, SC was clearly visible, showing the presence of normal corneocytes with
8 multiple cell layers, and its maturation was almost complete. We also examined the effect of a
9 moisturizing cream for barrier recovery on the SC repair, as compared to its vehicle. At 18 hours,
10 drug application induced a more evident increase of epidermal thickness, as compared to the
11 untreated TS model (Fig. 2a,b). Furthermore, claudin and filaggrin were re-expressed at 18 hours
12 only in treated TS models (Fig. 2a,c). At 24 hours, epidermal thickness, claudin and filaggrin
13 expression reverted to normal control only upon drug application (Fig. 2a,b,c). RCM confirmed the
14 barrier restoration and the activity of the drug that promotes skin regeneration (Fig. 2d). While 18
15 hours after TS control, skin surface displayed a homogeneous pattern with only few visible mature
16 corneocytes, in the presence of the drug, the corneocytes appeared larger, with a cytoplasm enriched
17 in organelles (that correlate with cell brightness), which are clear examples of recovery activity. At
18 24 hours cell contours became thicker and cells appeared to be bigger, as compared to untreated
19 samples.
20
21
22
23
24
25
26
27
28
29
30
31
32
33
34
35
36
37
38
39
40
41

42 **Skin barrier disruption by SDS alters cell-cell adhesion and terminal differentiation**

43
44
45 To better elucidate the molecular mechanism involved in barrier repair after chemical damage, we
46 exposed the organ cultures from healthy human skin to 2% SDS solution for 18 hours, and analyzed
47 the samples at different time points. Although SDS treatment fail to remove SC, skin barrier defects
48 were demonstrated by the altered expression of Dsg1 and by claudin (Fig. 3a,b). 18 hours after SDS
49 exposure, skin organ cultures re-expressed claudin and Dsg1 in a homogeneous pattern, which
50 became similar to control at 24 hours. By western blot analysis, claudin, filaggrin and Dsg3 were
51 strongly reduced after SDS treatment and were restored over time (Fig. 3c,d).
52
53
54
55
56
57
58
59
60

Proliferation increases during barrier recovery after SDS-induced damage

To address if SDS treatment induces keratinocytes apoptosis, we performed TUNEL assay. Similarly to TS, SDS application does not induce DNA fragmentation at all time points (Fig. S4a). Moreover, activated caspase-3 was not detected by western blot analysis (Fig. S4b). On the other hand, we observed a strong keratinocyte tendency to proliferate after SDS-induced damage (Fig. 3e). In particular, immediately after SDS treatment, the expression levels of Ki67 and P-Stat3 were respectively 3-fold and 42-fold more than the untreated controls (Fig. 3f). At 18 hours, Ki67 and P-Stat3 positive cell number showed a peak that progressively decreases in a time-dependent manner up to 36 hours.

RCM reveals morphological and functional aspects of barrier repair in SDS model

After SDS treatment, RCM revealed increased brightness of superficial layers and decreased interkeratinocyte brightness, suggesting a toxic damage to keratinocytes (Fig. 3g) (29). 18 and 24 hours after treatment, nuclei appeared pyknotic, while cell contours and junctions were poorly delineated. In particular, keratinocytes appeared detached from each other at 24 hours, and cell damage, corresponding to small bright polygonal keratinocytes (34) was found in the deeper layers. Conversely, cell shapes did not change significantly after 36 hours.

Skin barrier recovery after SDS or TS mimics inflammatory skin disease features

We also wanted to assess the immune response and cell activation consequent to barrier disruption. In human epidermis, LCs are in situ dendritic cells involved in immune functions and are characterized by the expression of CD1a (39) and other markers (40). SDS or TS induced a substantial increase in LCs starting from 18 hours post treatment (Fig. 4a,b,d,e). Similarly, keratinocytes displayed an “activation profile” typical of response to injuries or inflammatory skin

diseases, by showing increasing expression of keratin 16 and psoriasin (Fig. 4a,c,d,f). Indeed, keratin 16 expression is induced in hyperkeratotic lesions as well as in atopic dermatitis or psoriasis (41), and it has been recently shown to play a specific role in the regulation of immune response (42). Psoriasin, also indicated as S100A7, is overexpressed in hyperproliferative skin diseases, where it not only exhibits antimicrobial functions, but also induces immunomodulatory activities, including chemotaxis and cytokine/chemokine production (43). Therefore, these data indicates that our model can recapitulate the behavior of immune-inflammatory molecules in the context of skin conditions characterized by barrier disruption.

DISCUSSION

The alterations of the cornified layer imply barrier defects, including the transepidermal water loss (TEWL), dehydration, desquamation and loss of lipids contents, which are all found in several inflammatory skin diseases, such as atopic dermatitis and psoriasis (44). Given the frequency of such conditions (45, 46) and the necessity of ethical studies always closer to human skin physiology, it is important to have models that faithfully reproduce skin barrier defects. Indeed, they allow to elucidate several parameters, such as drug kinetic and penetration, infections and barrier repair after injuries.

Here, we investigated the *ex-vivo* skin barrier recovery by human skin organ cultures after acute barrier disruption achieved by physical or chemical treatment: tape stripping (TS), that physically removes the cornified layer, and SDS (sodium-dodecil-sulfate) application, which is known to be harsh on the SC and induces skin damage. Although these methods are widely used *in vivo*, the knowledge regarding the molecular mechanisms underlying barrier repair is still insufficient and sometimes controversial. Human *in vivo* studies often require mild aggression for ethical reasons and the results are frequently inconclusive because of a response with low significance, due to the absence of a real alteration of barrier function (4). On the other hand, barrier restoration studies are usually performed on transgenic animal models, which somehow show higher variability when compared to humans.

Therefore, in the present work, we analyze an alternative method to study skin barrier functionality by using *in vitro* models only. Moreover, the application of RCM confirms the feasibility of this innovative technique and the potential application in pharmacological studies regarding skin pathologies together with toxicological studies.

Our models allow maintaining human skin features *in vitro*, thus overcoming the inter-species variability. Our data report that both TS and SDS models applied on skin organ culture, recapitulate

1
2
3
4
5
6
7
8
9
10
11
12
13
14
15
16
17
18
19
20
21
22
23
24
25
26
27
28
29
30
31
32
33
34
35
36
37
38
39
40
41
42
43
44
45
46
47
48
49
50
51
52
53
54
55
56
57
58
59
60

the main histological features observed after barrier and epidermal injuries that have been previously analyzed by in vivo models (7).

Skin mechanical resistance is ensured by a scaffold of structural components, proteins involved in epidermal terminal differentiation and lipids (36). It has been established that the acute barrier perturbation induces a transitory reduction of the calcium levels in the stratum granulosum that lead to lower levels of involucrin, loricrin and profilaggrin (7). Our models confirmed that skin barrier disruption, either chemically or mechanically induced, involved both terminal differentiation protein alterations, such as involucrin, filaggrin, loricrin, and lower expression of intercellular junctions mediators, such as claudin and desmoglein. Indeed, after skin barrier disruption, there is a temporary imbalance between cornification and desquamation (47). This phenomena results in hyperkeratosis and parakeratosis, which ensure a rapid skin barrier repair (7), and act as regulatory mechanism that in turn stimulates basal layer proliferative kinetics (5). We observed not only high expression levels of Ki67, but also skin hyperplasia after injury. The presence of inflammatory-related marker modulation renders both TS and SDS models suitable for the study of the effect of immunomodulatory drugs in the context of skin barrier defects.

RCM enabled the monitoring of morphological changes occurring during the experiments without alteration of the tissue. It was possible to identify different dynamics in consequence of the application of mechanical (tape stripping) or chemical (SDS) barrier perturbation models. Upper layer removal induced a cellular activation able to restore the missing layers in approximately 36 hours passing through an initial thickening of the intermediate layers (spinosum and granulosum, presenting as honeycombed structure detectable on the top of the skin surface) followed by reintegration of corneocytes that appeared with a brighter and more granulous cytoplasm probably because of the epithelial activation. Interestingly, these physiological phenomena were accelerated by the application of a recovery cream, reducing the time required for corneocyte restoration of approximately one third (from 24 to 36 hours). In case of SDS application, an increased brightness

of corneocyte (probably for cytoplasmic clotting/cohortation) was visible immediately after, whereas appearance of bright basal keratinocytes, correlated with cytological damage and necrosis, was an 18-24 hours delayed event. Interestingly, the morphological changes documented by means of RCM were correlated with the immunohistochemical dynamics, suggesting the added value of a non-invasive technology to study the events occurring in an in vitro model. This means a faster approach that can be used as first non-invasive screening. Moreover, thanks to the knowledge obtained from the study of in vitro models, the morphological changes observed by means of RCM can be exported and compared to in vivo models, in order to gain more specific and biomolecular correlated information during clinical tests of skin topical products.

Conflict of interest

The authors declare no conflict of interest.

REFERENCES

1. Scheuplein R J, Blank I H. Permeability of the skin. *Physiol Rev* 1971; 51: 702-747.

2. Serre G, Mils V, Haftek M *et al.* Identification of late differentiation antigens of human cornified epithelia, expressed in re-organized desmosomes and bound to cross-linked envelope. *J Invest Dermatol* 1991; 97: 1061-1072.

3. Niessen C M. Tight junctions/adherens junctions: basic structure and function. *J Invest Dermatol* 2007; 127: 2525-2532.

4. Marionnet C, Bernerd F, Dumas A *et al.* Modulation of gene expression induced in human epidermis by environmental stress in vivo. *J Invest Dermatol* 2003; 121: 1447-1458.

5. Barthel D, Matthé B, Potten C S *et al.* Proliferation in murine epidermis after minor mechanical stimulation. Part 2. Alterations in keratinocyte cell cycle fluxes. *Cell Prolif* 2000; 33: 247-259.

6. Potten C S, Barthel D, Li Y Q *et al.* Proliferation in murine epidermis after minor mechanical stimulation. Part 1. Sustained increase in keratinocyte production and migration. *Cell Prolif* 2000; 33: 231-246.

7. de Koning H D, van den Bogaard E H, Bergboer J G *et al.* Expression profile of cornified envelope structural proteins and keratinocyte differentiation-regulating proteins during skin barrier repair. *Br J Dermatol* 2012; 166: 1245-1254.

8. Escobar-Chávez J J, Merino-Sanjuán V, López-Cervantes M *et al.* The tape-stripping technique

as a method for drug quantification in skin. J Pharm Pharm Sci 2008; 11: 104-130.

9. Pinkus H. Examination of the epidermis by the strip method of removing horny layers. I. Observations on thickness of the horny layer, and on mitotic activity after stripping. J Invest Dermatol 1951; 16: 383-386.

10. Reaven E P, Cox A J. Behavior of adult human skin in organ culture. II. Effects of cellophane tape stripping, temperature, oxygen tension, pH and serum. J Invest Dermatol 1968; 50: 118-128.

11. Wang C Y, Maibach H I. Why minimally invasive skin sampling techniques? A bright scientific future. Cutan Ocul Toxicol 2011; 30: 1-6.

12. Klang V, Schwarz J C, Lenobel B et al. In vitro vs. in vivo tape stripping: validation of the porcine ear model and penetration assessment of novel sucrose stearate emulsions. Eur J Pharm Biopharm 2012; 80: 604-614.

13. Holmgaard R, Benfeldt E, Nielsen J B. Percutaneous Penetration – Methodological Considerations. Basic Clin Pharmacol Toxicol 2014; 115: 101-109.

14. Videmont E, Mariani C, Vidal S *et al.* Characterization of the canine skin barrier restoration following acute disruption by tape stripping. Vet Dermatology 2012; 23: 103-109.

15. Nishifuji K, Yoon J S. The stratum corneum: the rampart of the mammalian body. Vet Dermatol 2013; 24: 60-72.

16. Barbero A M, Frasc H F. Pig and guinea pig skin as surrogates for human in vitro penetration

studies: a quantitative review. *Toxicol In Vitro* 2009; 23: 1-13.

17. Pellacani G, Longo C, Malvehy J *et al.* In vivo confocal microscopic and histopathologic correlations of dermoscopic features in 202 melanocytic lesions. *Arch Dermatol* 2008; 144: 1597-1608.

18. Pellacani G, Guitera P, Longo C *et al.* The impact of in vivo reflectance confocal microscopy for the diagnostic accuracy of melanoma and equivocal melanocytic lesions. *J Invest Dermatol* 2007; 127: 2759-2765.

19. Guitera P, Menzies S W, Longo C *et al.* In vivo confocal microscopy for diagnosis of melanoma and basal cell carcinoma using a two-step method: analysis of 710 consecutive clinically equivocal cases. *J Invest Dermatol* 2012; 132: 2386-2394.

20. Wilson T. Confocal Microscopy. In: *Confocal Microscopy*, ed. San Diego: Academic Press. 1990.

21. Pawley J B. *Handbook of Biological Confocal Microscopy*, 2nd Edition, ed. New York: Plenum Press. 2009.

22. Webb R H. Confocal optical microscopy. *Rep Prog Phys* 1996; 59: 427-471.

23. Rajadhyaksha M, Grossman M, Esterowitz D *et al.* In vivo confocal scanning laser microscopy of human skin: melanin provides strong contrast. *J Invest Dermatol* 1995; 104: 946-952.

24. Calzavara-Pinton P, Longo C, Venturini M *et al.* Reflectance confocal microscopy for in vivo

1
2
3 skin imaging. Photochem Photobiol 2008; 84: 1421-1430.
4
5

6
7 25. Gonzalez S, Rajadhyaksha M, Rubinstein G *et al*. Confocal imaging of sebaceous gland
8 hyperplasia in vivo to assess efficacy mechanism of pulsed dye laser treatment. Lasers Surg Med
9 1999; 25: 8-12.
10
11

12
13
14
15
16 26. Aghassi D, Anderson R R, Gonzales S. Time-sequence histologic imaging of laser-treated
17 cherry angiomas using in vivo confocal microscopy. J Am Acad Dermatol 2000; 43: 37-41.
18
19

20
21
22
23 27. Aghassi D, Anderson R R, Gonzalez S. Confocal laser microscopic imaging of actinic keratoses
24 in vivo: a preliminary report. J Am Acad Dermatol 2000; 43: 42-48.
25
26

27
28
29 28. Gonzalez S, Gonzales E, White W M *et al*. Allergic contact dermatitis. Correlation in vivo
30 confocal imaging to routine histology. J Am Acad Dermatol 1999; 40: 708-713.
31
32

33
34
35
36 29. Astner S, González E, Cheung A C *et al*. Non-invasive evaluation of the kinetics of allergic and
37 irritant contact dermatitis. J Invest Dermatol 2005; 124: 351-359.
38
39

40
41
42
43 30. Nori S, Rius-Diaz F, Cuevas J *et al*. Sensitivity and specificity of reflectance-mode confocal
44 microscopy for in vivo diagnosis of basal cell carcinoma: a multicenter study. J Am Acad Dermatol
45 2004; 51: 923-930.
46
47

48
49
50
51 31. Pellacani G, Cesinaro A M, Seidenari S. Reflectance-mode confocal microscopy of pigmented
52 skin lesions--improvement in melanoma diagnostic specificity. J Am Acad Dermatol 2005; 53: 979-
53 985.
54
55
56
57
58
59
60

32. Manfredini M, Mazzaglia G, Ciardo S *et al.* Does skin hydration influence keratinocyte biology? In vivo evaluation of microscopic skin changes induced by moisturizers by means of reflectance confocal microscopy. *Skin Res Technol* 2013; 19: 299-307.

33. de Koning H D, Kamsteeg M, Rodijk-Olthuis D *et al.* Epidermal Expression of Host Response Genes upon Skin Barrier Disruption in Normal Skin and Uninvolved Skin of Psoriasis and Atopic Dermatitis Patients *J Invest Dermatol* 2011; 131: 263–266.

34. Ulrich M, Rüter C, Astner S *et al.* Comparison of UV-induced skin changes in sun-exposed vs. sun-protected skin- preliminary evaluation by reflectance confocal microscopy. *Br J Dermatol* 2009; 161 Suppl 3: 46-53.

35. Draelos Z D. New treatments for restoring impaired epidermal barrier permeability: skin barrier repair creams. *Clin Dermatol* 2012; 30: 345-348.

36. Candi E, Schmidt R, Melino G. The cornified envelope: a model of cell death in the skin. *Nat rev mol cell boil* 2005; 6: 328-340.

37. Igawa S, Kishibe M, Honma M *et al.* Aberrant distribution patterns of corneodesmosomal components of tape-stripped corneocytes in atopic dermatitis and related skin conditions (ichthyosis vulgaris, Netherton syndrome and peeling skin syndrome type B). *J Dermatol Sci* 2013; 72: 54-60.

38. Yamamoto-Tanaka M, Makino T, Motoyama A *et al.* Multiple pathways are involved in DNA degradation during keratinocyte terminal differentiation. *Cell Death Dis* 2014; 5: e1181.

39. Mizumoto N., Takashima A. CD1a and langerin: acting as more than Langerhans cell markers.

Clin Invest 2004; 113: 658–660.

40. Zaba L C, Krueger J G, Lowes M A. Resident and inflammatory dendritic cells in human skin. J Invest Dermatol 2009; 129: 302–308.

41. Leigh I M, Navsaria H, Purkis P E *et al.* Keratins (K16 and K17) as markers of keratinocyte hyperproliferation in psoriasis in vivo and in vitro. Br J Dermatol 1995; 133: 501-511.

42. Lessard J C, Piña-Paz S, Rotty J D *et al.* Keratin 16 regulates innate immunity in response to epidermal barrier breach. Proc Natl Acad Sci U S A 2013; 110: 19537-19542.

43. Hattori F, Kiatsurayanon C, Okumura K *et al.* The antimicrobial protein S100A7/psoriasin enhances the expression of keratinocyte differentiation markers and strengthens the skin's tight junction barrier. Br J Dermatol 2014; 171: 742-753.

44. Segre J A. Epidermal barrier formation and recovery in skin disorders. J Clin Invest 2006; 116: 1150-1158.

45. Naldi L, Mercuri S R. Epidemiology of comorbidities in psoriasis. Dermatol Ther 2010; 23: 114-118.

46. Boguniewicz M, Leung D Y. Atopic dermatitis: a disease of altered skin barrier and immune dysregulation. Immunol Rev 2011; 242: 233-246.

47. Elias P M, Ahn S K, Denda M *et al.* Modulations in epidermal calcium regulate the expression of differentiation-specific marker. J Invest Dermatol 2002; 119: 1128-1136.

LEGENDS FOR ILLUSTRATIONS

Figure 1. Tape stripping alters terminal differentiation, cellular junctions, lipid content and induces a rapid increase of proliferation. (a) Red Oil O and immunohistochemical staining of filaggrin, loricrin, claudin, Ki67 and pSTAT-3 in skin organ culture at different time points after TS. Scale bar: 200 μ m; (b) Staining intensity evaluation of Red Oil O, filaggrin, loricrin, claudin expression as described in M&M; (c) Expression of filaggrin, Dsg 1 and involucrin in skin organ culture at different time points after TS treatment, by Western blotting analysis. Vinculin was used as loading control; (d) Relative intensity of the results in (c) was quantified by laser scanner densitometry and analyzed by ImageJ software. (e) Bar graph showing Ki67 and P-Stat3 positive cells in (a); (f) RCM images of skin organ cultures at 0, 18, 24 and 36 hours after TS treatment. Any single image visualizes and area of 0.8 by 0.8 mm (1000 x 1000 pixels, grey-scale of 256 pixels) enabling a lateral resolution of approximately 1 μ m.

Figure 2. RCM confirms the full SC restoration of the barrier recovery cream in TS model. (a) H&E, immunohistochemical staining of filaggrin and immunofluorescence staining of claudin in skin organ cultures at 18 and 24 hours after TS treatment w/o the use of a barrier recovery cream. Scale bar: 200 μ m; (b) Epidermal thickness, at different time points after application of barrier recovery cream, was measured by ImageJ software; (c) Staining intensity evaluation of filaggrin and claudin expression as described in M&M; (d) RCM images of skin organ culture in (a). Any single image visualizes and area of 0.8 by 0.8 mm (1000 x 1000 pixels, grey-scale of 256 pixels) enabling a lateral resolution of approximately 1 μ m.

Figure 3. SDS treatment alters barrier and epidermal homeostasis, filaggrin expression and cellular junctions. (a) H&E and immunofluorescence staining of claudin and dsg1 in skin organ cultures at different times after 2% SDS treatment. Scale bar: 200 μ m; (b) Staining intensity evaluation of the

1
2
3 results in (a) as described in M&M; (c) Expression of filaggrin, claudin, and Dsg3 in human skin
4 organ cultures at different time points after SDS treatment, by Western blotting analysis. β -actin
5 was used as control; (d) Relative intensity of the results in (c) was quantified by laser scanner
6 densitometry and analyzed by ImageJ software. (e) Ki67 and pSTAT-3 immunohistochemical
7 staining of skin human organ cultures at different time points after SDS treatment. Scale bar: 200
8 μ m; (f) Bar graph showing Ki67 and P-Stat3 positive cells in (e); (g) RCM image of skin organ
9 cultures at 0, 18, 24 and 36 hours after 2%SDS treatment. Any single image visualizes and area of
10 0.8 by 0.8 mm (1000 x 1000 pixels, grey-scale of 256 pixels) enabling a lateral resolution of
11 approximately 1 μ m.
12
13
14
15
16
17
18
19
20
21
22
23

24
25 Figure 4. Barrier restoration after tape stripping or SDS treatment involves dendritic cell infiltration
26 and keratinocyte activation. CD1a, keratin 16 and psoriasin immunohistochemical staining of skin
27 human organ cultures at different time points after TS (a) or SDS treatment (d). Scale bar: 200 μ m;
28 (b) Evaluation of CD1a positive cells in (a) as percentage, normalized to the number of
29 hematoxylin-positive nuclei in the epidermis. (c) Staining intensity evaluation of keratin 16 and
30 psoriasin expression, as described in M&M. (D) Staining intensity evaluation of the results in (C),
31 as described in M&M.
32
33
34
35
36
37
38
39
40
41
42

43 Figure S1. Tape stripping (TS) and SDS model set up. Skin organ cultures were generated from
44 healthy skin obtained from surgery waste materials. For the TS model, repeated 3M adhesive tape
45 applications and removal were applied on total skin before performing punch biopsies. These were
46 maintained in air-liquid interface and analyzed at different time points. For the SDS model, skin
47 punch biopsies were treated with 2% SDS and incubated at 4°C for 18 hours before starting
48 culturing in air-liquid interface. They were analyzed at different time points after SDS treatment.
49
50
51
52
53
54
55
56
57
58
59
60

1
2
3
4
5
6
7
8
9
10
11
12
13
14
15
16
17
18
19
20
21
22
23
24
25
26
27
28
29
30
31
32
33
34
35
36
37
38
39
40
41
42
43
44
45
46
47
48
49
50
51
52
53
54
55
56
57
58
59
60

Figure S2. Tape stripping induces total SC removal. (a) H&E staining of skin organ culture at different time points after 40, 60 or 100 tape applications. Scale bar: 200 μ m. For all comparisons in bar graphs, epidermal thickness, at 0h (b) and after 100 tape application at different time points (c), was measured by ImageJ software.

Figure S3. Evaluation of apoptosis in TS model. TUNEL assay (a) and caspase-3 expression by Western blotting analysis (b) in skin organ culture at different time points after TS treatment. Vinculin was used as loading control. Relative intensity of Western Blotting results was quantified by laser scanner densitometry and analyzed by ImageJ software.

Figure S4. Evaluation of apoptosis in SDS model. TUNEL assay (a) and caspase-3 expression by Western blotting analysis (b) in skin organ culture at different time points after SDS treatment. Vinculin was used as loading control. Relative intensity of Western Blotting results was quantified by laser scanner densitometry and analyzed by ImageJ software.

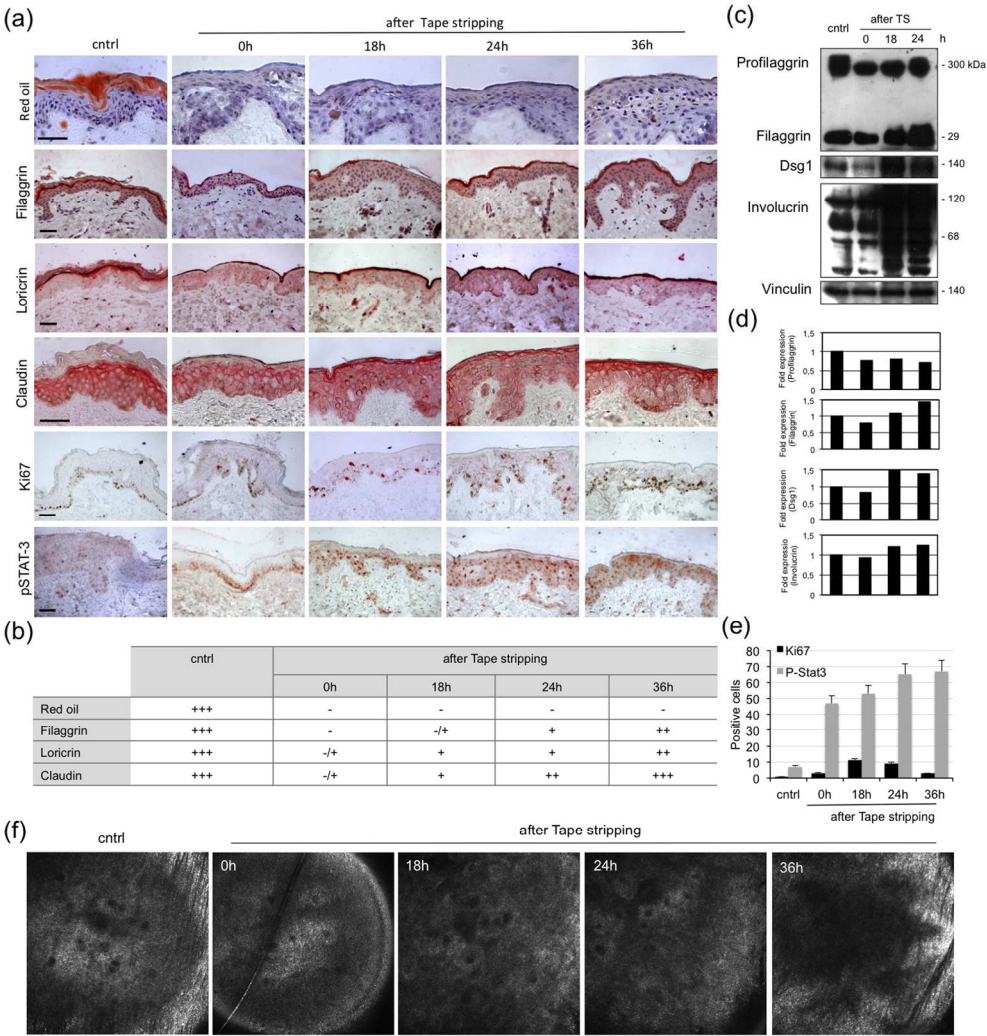


Figure 1. Tape stripping alters terminal differentiation, cellular junctions, lipid content and induces a rapid increase of proliferation.

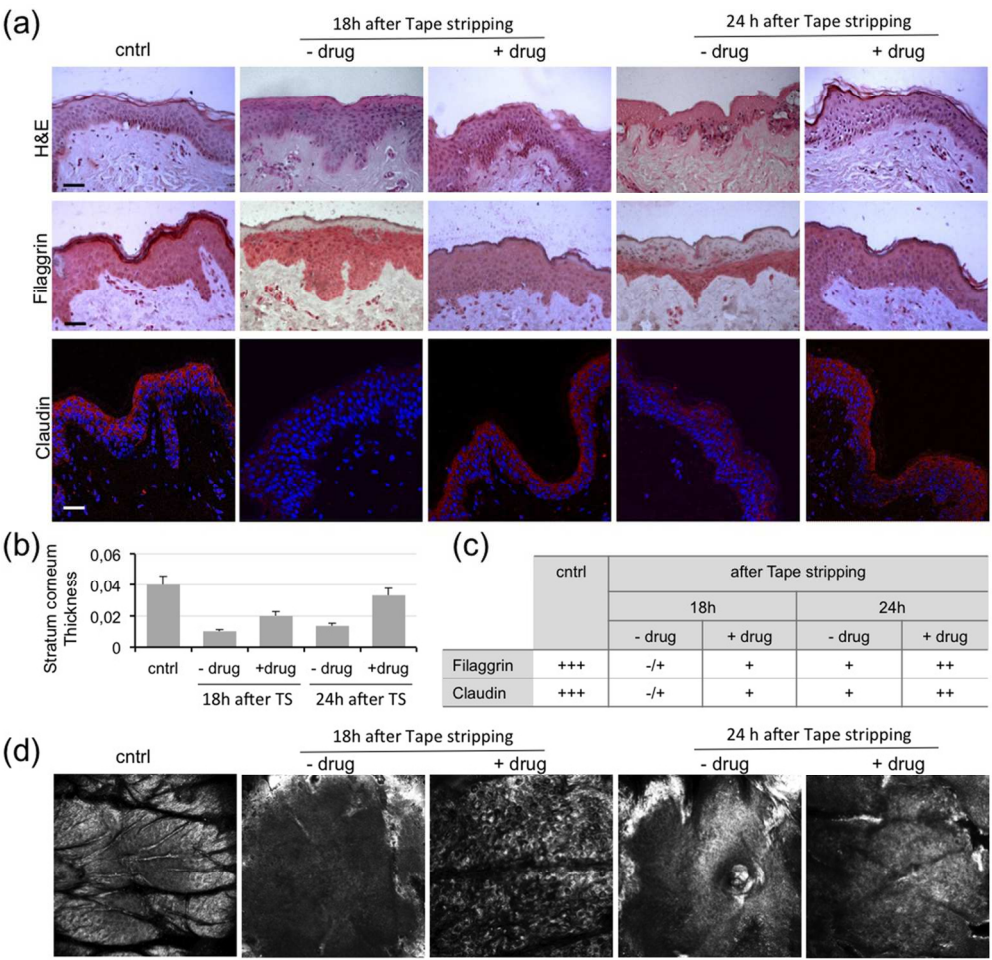


Figure 2. RCM confirms the full SC restoration of the barrier recovery cream in TS model.
116x112mm (300 x 300 DPI)

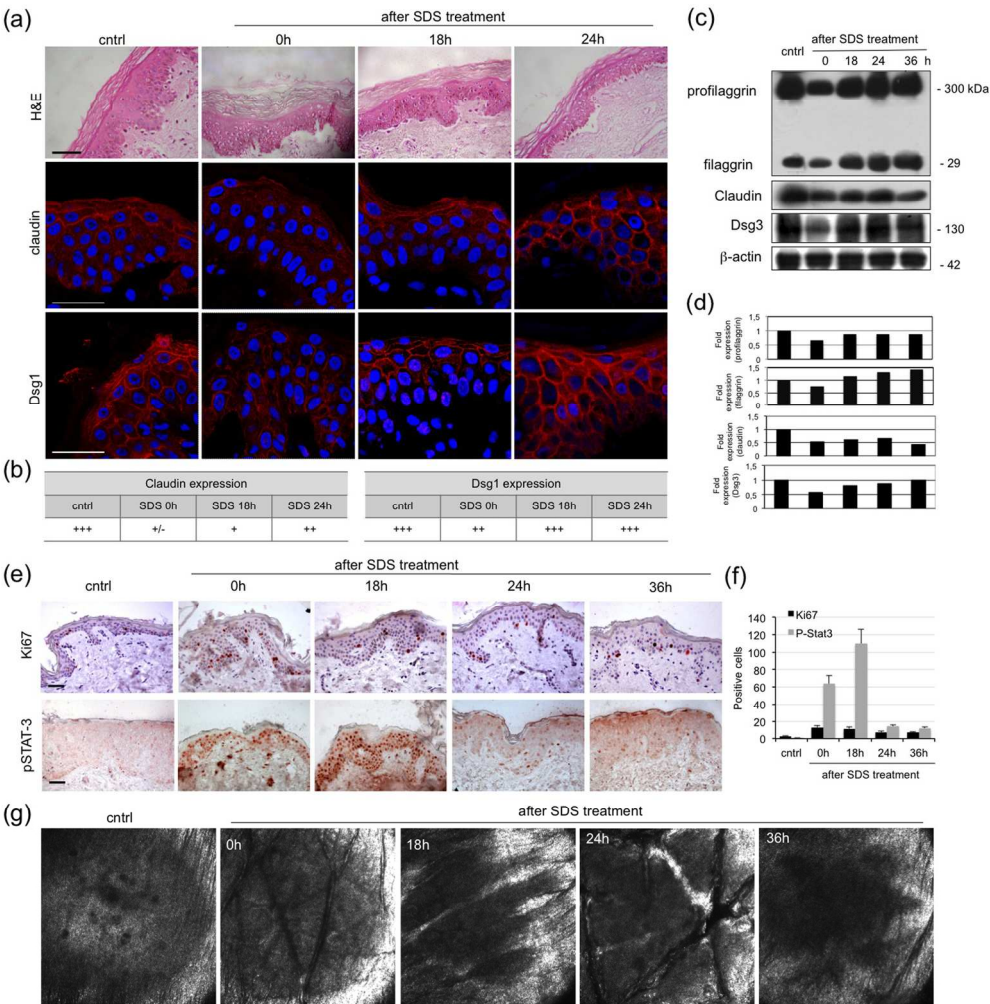


Figure 3. SDS treatment alters barrier and epidermal homeostasis, filaggrin expression and cellular junctions

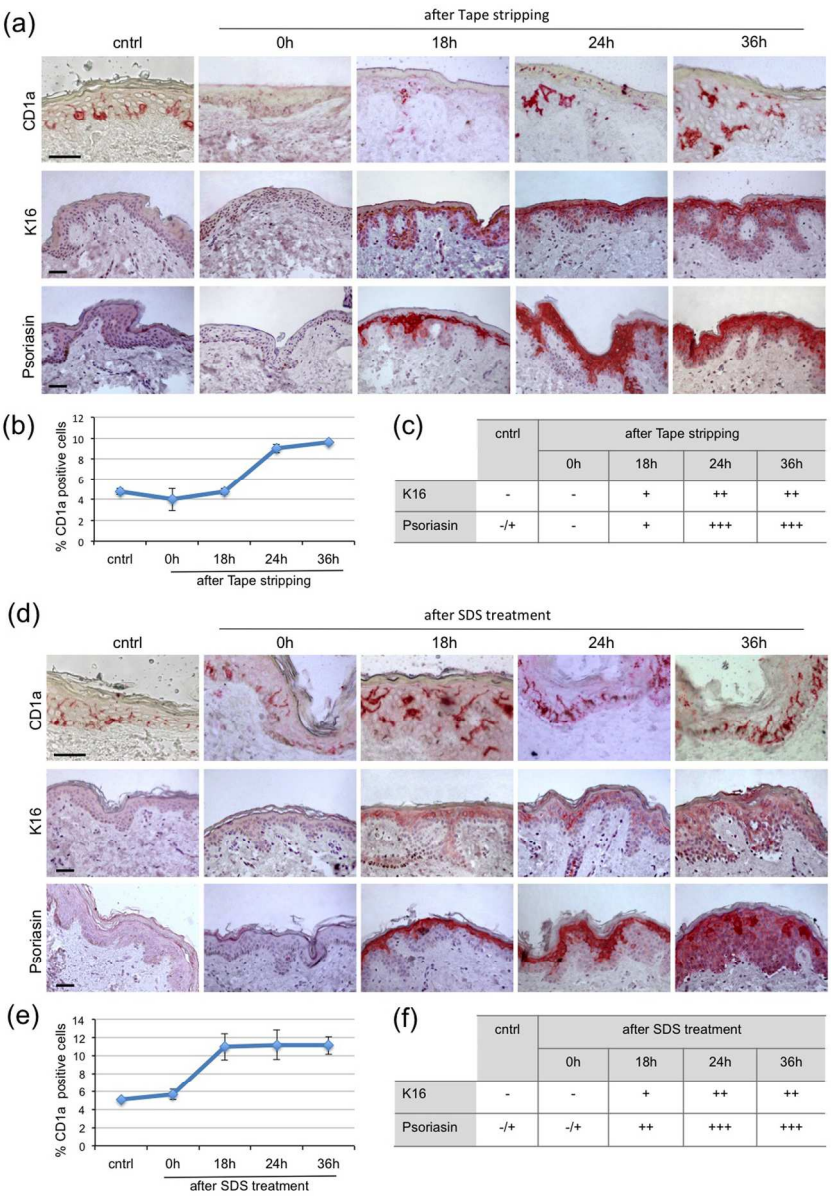


Figure 4. Barrier restoration after tape stripping or SDS treatment involves dendritic cell infiltration and keratinocyte activation.

171x244mm (300 x 300 DPI)

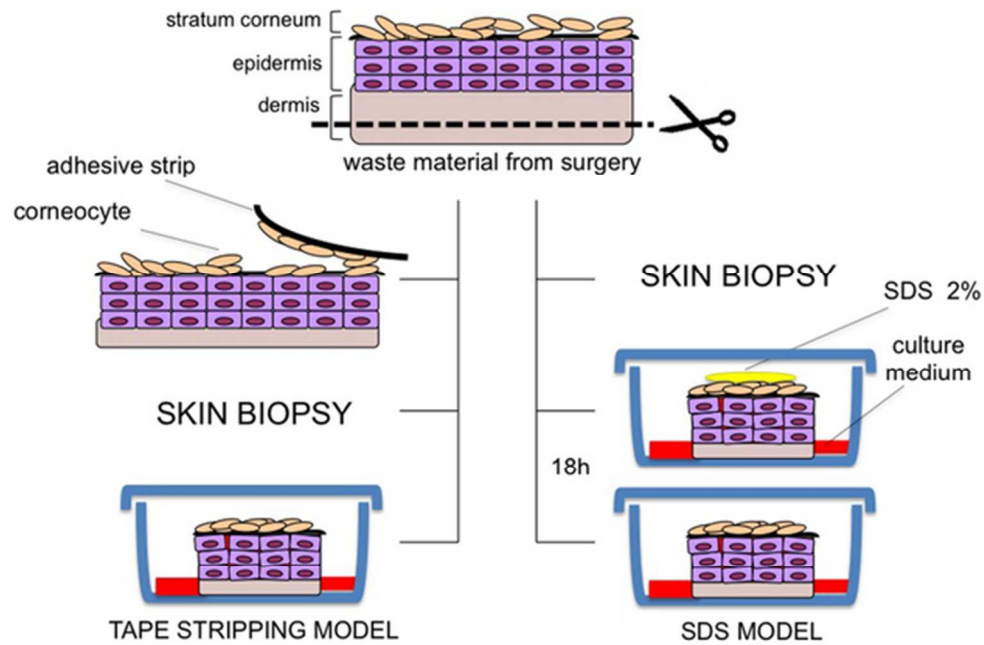


Figure S1. Tape stripping (TS) and SDS model set up. Skin organ cultures were generated from healthy skin obtained from surgery waste materials. For the TS model, repeated 3M adhesive tape applications and removal were applied on total skin before performing punch biopsies. These were maintained in air-liquid interface and analyzed at different time points. For the SDS model, skin punch biopsies were treated with 2% SDS and incubated at 4°C for 18 hours before starting culturing in air-liquid interface. They were analyzed at different time points after SDS treatment.

54x37mm (300 x 300 DPI)

1
2
3
4
5
6
7
8
9
10
11
12
13
14
15
16
17
18
19
20
21
22
23
24
25
26
27
28
29
30
31
32
33
34
35
36
37
38
39
40
41
42
43
44
45
46
47
48
49
50
51
52
53
54
55
56
57
58
59
60

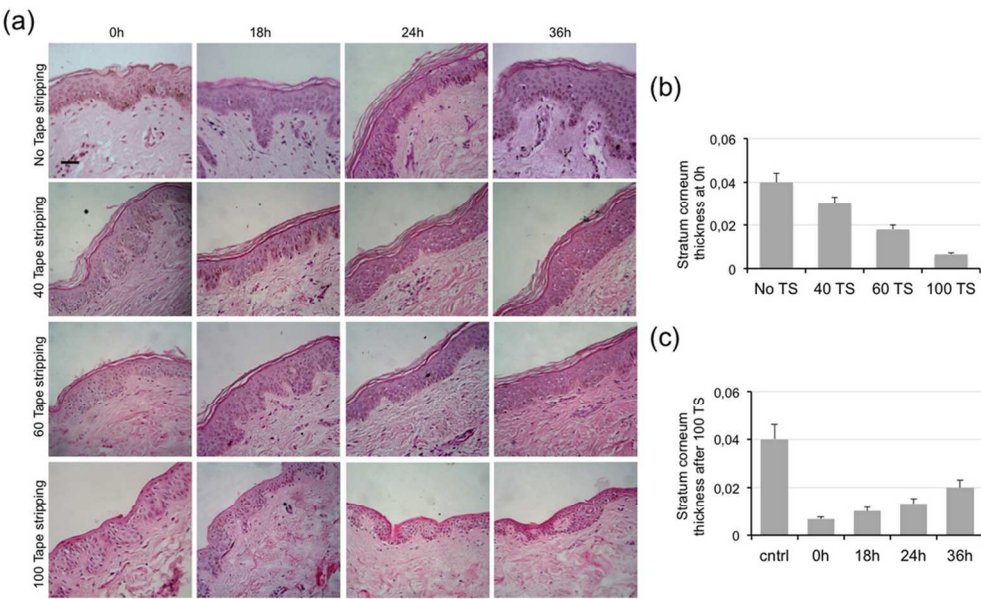


Figure S2. Tape stripping induces total SC removal. (a) H&E staining of skin organ culture at different time points after 40, 60 or 100 tape applications. Scale bar: 200 μ m. For all comparisons in bar graphs, epidermal thickness, at 0h (b) and after 100 tape application at different time points (c), was measured by ImageJ software.
101x61mm (300 x 300 DPI)

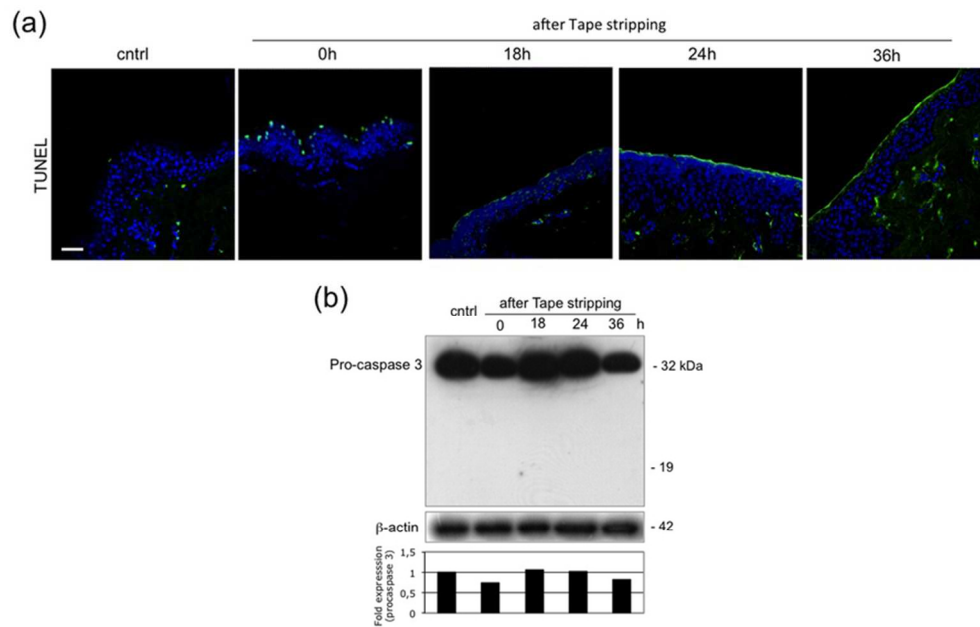


Figure S3. Evaluation of apoptosis in TS model. TUNEL assay (a) and caspase-3 expression by Western blotting analysis (b) in skin organ culture at different time points after TS treatment. Vinculin was used as loading control. Relative intensity of Western Blotting results was quantified by laser scanner densitometry and analyzed by ImageJ software.

76x49mm (300 x 300 DPI)

1
2
3
4
5
6
7
8
9
10
11
12
13
14
15
16
17
18
19
20
21
22
23
24
25
26
27
28
29
30
31
32
33
34
35
36
37
38
39
40
41
42
43
44
45
46
47
48
49
50
51
52
53
54
55
56
57
58
59
60

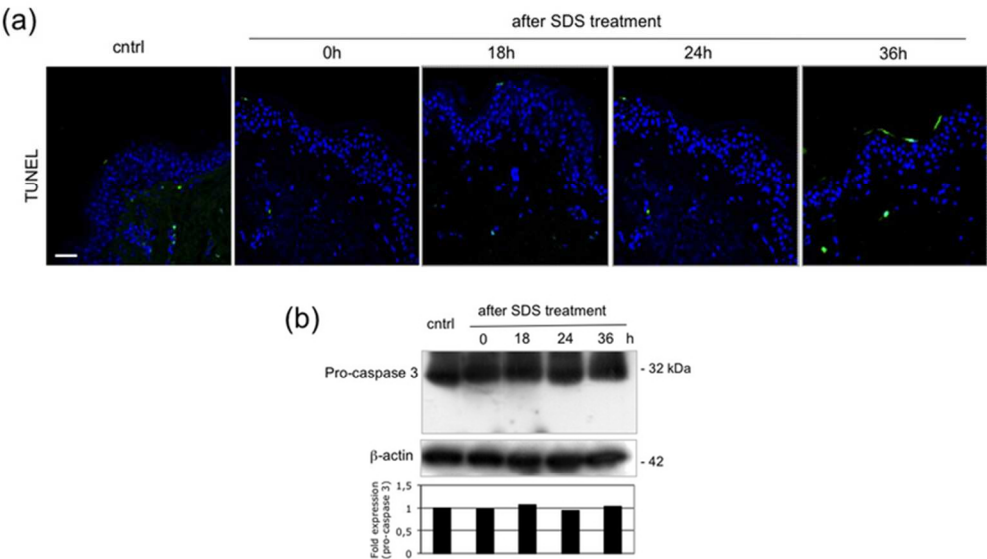


Figure S4. Evaluation of apoptosis in SDS model. TUNEL assay (a) and caspase-3 expression by Western blotting analysis (b) in skin organ culture at different time points after SDS treatment. Vinculin was used as loading control. Relative intensity of Western Blotting results was quantified by laser scanner densitometry and analyzed by ImageJ software.

69x39mm (300 x 300 DPI)